Histological and ultrastructural studies on the effect of *Cassia alata* methanolic leaf extracts against chemically induced lung adenocarcinoma in rats

[*Estudos histológicos e ultraestruturais sobre o efeito dos extratos metanólicos das folhas de Cassia alata contra o adenocarcinoma pulmonar induzido quimicamente em ratos*]

A.S. *Fathalla*[1] , M.A. *Ibrahim*[1*] , S.R. *Mohamed*[1] , M.A. *Dkhil*[1,2] , F.A. *Thagfan*[3] ,
R. *Abdel-Gaber* [4] , D. *Soliman*[1]

[1]Zoology and Entomology Department, Faculty of Science, Helwan University, Egypt
[2]Applied Science Research Center, Applied Science Private University, Amman, Jordan
[3] Department of Biology, College of Science, Princess Nourah bint Abdulrahman University, Riyadh, Saudi Arabia
[4] Department of Zoology, College of Science, King Saud University, Riyadh, Saudi Arabia

ABSTRACT

The present work aims to evaluate anticancer performance of *Cassia alata* methanolic leaf extracts (CMLE) in ethyl carbamate-stimulated lung adenocarcinoma (LAD) in differentiation to the function of Cisplatin (CIPL). Rats were divided into four groups: (1) control (CONT), (2) lung-adenocarcinoma (LAD) injected intra-peritoneally with 1g/kg ethyl carbamate once weekly for a month, (3) LAD+CMLE administered 500 mg/kg CMLE orally for the last two months of the experiment, and (4) LAD+CIPL treated group, injected 2.5 mg/kg Cisplatin intraperitoneally once weekly for the last two months of the experiment. Light and electron microscopic examinations revealed adenocarcinoma development in terminal bronchiole besides some histopathological changes in the LAD group such as atypical, exaggerated collagen fibers, increment of mucinous content, and increasing of PCNA positive immunoreactivity whereas electron microscopy investigation exposed that papillary adenocarcinoma originated from Clara cells in the LAD group. The LAD+CMLE treated group showed no tumor masses and nearly all with normal lung histology. It also recovered the normal ultrastructure of bronchiolar Clara cells. CMLE treatment offers a new alternative cure with less toxicity than Cisplatin for lung cancer therapy. Hence, CMLE would be employed as a novel supply of anti-cancer compounds combating lung cancer.

Keywords: *Cassia alata*, Ethyl carbamate, lung adenocarcinoma, Cisplatin, clara cells, immunohistochemistry

RESUMO

O presente trabalho tem como objetivo avaliar o desempenho anticâncer dos extratos metanólicos das folhas de Cassia alata (CMLE) em adenocarcinoma pulmonar estimulado por carbamato de etila (LAD) em diferenciação com a função da cisplatina (CIPL). Os ratos foram divididos em quatro grupos: (1) controle (CONT), (2) adenocarcinoma de pulmão (LAD) injetado intraperitonealmente com 1g/kg de carbamato de etila uma vez por semana durante um mês, (3) LAD+CMLE administrado 500 mg/kg de CMLE por via oral nos últimos dois meses do experimento e (4) grupo tratado com LAD+CIPL, injetado 2,5 mg/kg de cisplatina intraperitonealmente uma vez por semana nos últimos dois meses do experimento. Os exames de microscopia de luz e eletrônica revelaram o desenvolvimento de adenocarcinoma no bronquíolo terminal, além de algumas alterações histopatológicas no grupo LAD, como fibras de colágeno atípicas exageradas, aumento do conteúdo mucinoso e aumento da imunorreatividade positiva para PCNA, enquanto a investigação de microscopia eletrônica revelou que o adenocarcinoma papilar se originou das células Clara no grupo LAD. O grupo tratado com LAD+CMLE não apresentou massas tumorais e quase apresentou histologia pulmonar normal. Ele também recuperou a ultraestrutura normal das células de Clara bronquiolares. O tratamento com CMLE oferece uma nova alternativa de cura com menos toxicidade do que a cisplatina para a terapia do câncer de pulmão. Portanto, o CMLE seria empregado como um novo suprimento de compostos anticancerígenos para combater o câncer de pulmão.

Palavras-chave: Cassia alata, Carbamato de etila, adenocarcinoma de pulmão, cisplatina, células de clara, imunohistoquímica

INTRODUCTION

According to Egypt's National Population-Based Registry Program (NCRPE), lung cancer, along with breast, brain, liver, and urinary bladder cancer, is one of the five most common types of cancer (Hamzawy *et al.*, 2022). Adenocarcinoma is the most common type of lung cancer, with 6,538 people (4,851 men and 1,687 women) newly diagnosed in Egypt in 2020 (Sung *et al.*, 2021).

Non-small cell lung cancer (NSCLC) and small cell lung cancer (SCLC) are the two most common histological forms of lung cancer, accounting for around 85% and 15% of cases, respectively. Surgery, chemotherapy, radio-therapy, and immuno-therapy are now accessible (Wilcox *et al.*, 2008; Ju *et al.*, 2012, Travis, 2012).

Ethyl carbamate, often known as urethane, is a carbamic acid ester that has been detected as a byproduct of fermented beverages and foods. Because of unwitting fermentation through the storing or making of fermented beverages and foods, it is greatly spread (Dennis *et al.*, 1989). Because of formation of vinyl carbamate, an active metabolite, Ethyl carbamate produced malignant lesions in various body locations. Continual exposure to ethyl carbamate which is found in fermented beverages and foods enlarges lung cancer risk through irreversible malfunction of mitochondria and increment of cellular mitotic activity (Hamzawy and Abo Youssef, 2015).

Cisplatin is a well-known platinum-based chemotherapeutic drug that is effective against a variety of cancers such as lung cancer, ovarian cancer, and breast cancer (Santarpia *et al.*, 2017). Cisplatin destroys cells in two distinct ways. For starters, it can cause cytoplasmic mitochondrial apoptosis. Second, it enters the cell membrane for hydration, substituting one chloric ion with one water molecule, and then enters the nucleus to attach to a single nitrogen on a DNA nucleotide. Ethyl carbamate, often known as urethane, is a carbamic acid ester that has been detected as a byproduct of fermented beverages and foods. After that, one molecule of water replaces the second chloric ion, causing it to bind to a second nucleotide (Tanriverdi *et al.*, 2007). Cisplatin binds with DNA, forming covalent adducts with purine DNA bases, and this reaction

is the main cause of cisplatin's cytotoxic effect (Yousef *et al.*, 2009). Cisplatin therapy causes a number of toxic side effects, in heart, kidney and liver (Jongh *et al.*, 2003; Al-Majed, 2007).

Chemotherapy containing Platinum is still the recommended treatment for most progressive non-small cell lung-cancer (NSCLC) patients (Ibrahim *et al.*, 2014). The creation of a more effective and safe alternative treatment strategy is necessary due to the excessive toxicity and chemoresistance linked to traditional chemotherapies, which lower the success rates of the present chemotherapeutic regimen (Swetha *et al.*, 2022). Numerous studies suggest that natural polyphenols work through a variety of molecular mechanisms to combat different types of cancer in either a chemo-preventive or chemotherapeutic way (Zhou *et al.*, 2019).

The family Fabaceae is considered the second largest widespread in the plant kingdom. It includes a big number of phytochemicals (saponins, alkaloids, flavonoids, phenolic acids, lectins, and carotenoids) with an assortment of health advantages, most notably anti-cancer activity (Usman *et al.*, 2022).

Cassia alata is the commonly used term for *Senna alata*. It is a fundamental medical shrub inside the Fabaceae family, Fabales order (Adedayo *et al.*, 2001). *C. alata* contains a variety of bioactive chemical compounds, including phenolics (aloe emodin, glycosides, chrysaphanol, rhein and kaempferol,), fatty acids (oleic, palmitic, and linoleic acids), anthraquinones (alatinone and alatonal), steroids, and terpenoids (sitosterol, stigmasterol and campesterol) (Liu *et al.*, 2009; Mohamed *et al.*, 2023). These secondary metabolites have been manifested to have a wide variety of biological activities (Fernand *et al.*, 2011).

C. alata leaf has been shown to contain phenolics and to have cytotoxic effect against cancer cells. Chrysoeriol, kaempferol, quercetin, palmitic acid, stearic acid, and other important chemical compounds are present, the bulk of these compounds have been found to have cytotoxic and anti-inflammatory effect against lung-cancer (Levy and Lewis, 2011; Olarte *et al.*, 2013).

858

Arq. Bras. Med. Vet. Zootec., v.75, n.5, p.857-871, 2023

This study aimed to investigate the effect of *C. alata* extracts against chemically induced lung adenocarcinoma in rats.

MATERIALS AND METHODS

Ethyl Carbamate: 99.0 percent, Sigma-Aldrich product, linear formulation, $NH_2COOC_2H_5$. Cisplatin: (1 mg/mL) (MYLAN). Other chemicals were purchased from El-Gomhoria Co. in Cairo, Egypt.

Fresh *C. alata* leaves were collected during July 2021 at Cairo University's Agriculture Farm, dried at room temperature in the shade, and milled to a soft powder. Methanol was used to extract 2 kg of the powder and then concentrated under reduced pressure at 40 °C. The methanolic extract remnant (22.57 percent) was dried using RE-2010 rotary evaporator (BIOBASE, China) at 40 °C. The collected components were kept until usage at -20 °C (Ali *et al*., 2017).

Adult albino rats (40 male rats, 150±20 g, 8-9 weeks old) were attained from Egypt's New Veterinary Office. Rats were housed in cages under condition of 12-hour light/dark cycles in a temperature-monitored setting. During the experiment, water and food were freely offered. The experiment was agreed to by the ethics committee of the Institutional Animal Care and Use Committee for Laboratory Animals at Zoology Department, Science Faculty, Helwan University (Approval number: HU-IACUC/Z/MI1101-23).

The rats were grouped into four main groups (10 rats for each) as follows:

Group 1- Control (CONT) group: rats received intraperitoneal injections of phosphate buffered solution for 7 months.

Group 2- Lung adenocarcinoma (LAD) group: Animals served as the carcinogenic non-treated group. For induction of lung cancer, for a month, rats were intraperitoneally injected with 1g/kg/rat/week ethyl carbamate (Janker *et al*., 2018). Thirty adult male albino rats were given intra-peritoneal injections of ethyl carbamate (1g/kg) once weekly. Lung cancer developed after a 5-month latency period following the initial urethane injection. This group consists of ten rats that were left untreated for two months.

Group 3- LAD+CMLE treated group: Rats were orally administered with CMLE (500 mg/kg) daily (Onyegeme-Okerenta *et al*., 2017). Treatment began after the fifth month and continued until the experiment was completed.

Group 4- LAD+CIPL treated group: Lung cancer rats were injected intraperitoneally with Cisplatin (2.5 mg/kg/week) (Jafri *et al*., 2010). Treatment began after the fifth month and continued until the trial was completed.

At the end of the experiment, rats were sacrificed using isoflurane anesthesia at concentration of 6% and excised their lungs rapidly and cleansed in saline. Each lung was divided into two sections, one for histopathologic staining in neutral-buffered formalin at concentration of 10% and the other fixed in glutaraldehyde for transmission electron microscope of bronchiolar Clara cells.

The fixed lung specimens were processed for paraffin section preparation at thickness of 5 μm (Spencer and Bancroft, 2013). The slides were observed after staining by a light microscope of LEICA model and taken pictures by a Zeiss camera. For general histopathological observation of lung tissue, we used hematoxylin and eosin stain (H&E) (Bancroft and Layton, 2019). It was also used to assess lung bronchiolar wall thickness, alveolar lumen diameter, and inflammatory score. We used a semi-quantified inflammatory score, with grades 0 denoting no inflammation, 1 implying minimal inflammatory cells in some microscope fields, 2 revealing mild inflammation with an influx of a ring of cells 1 cell layer deep, 3 indicating moderate inflammation with a ring of cells 2-4 cells deep, and 4 inferring severe inflammation with a ring of cells > 4 cells deep (Dong *et al*., 2012).

ImageJ analysis software (NIH, version, 1.46, LOCI, University of Wisconsin, USA) was used to measure and statistically analyze the bronchiolar wall thickness (μm) and alveolar lumen diameter (μm). The mean bronchiolar wall thickness, alveolar lumen diameter, and inflammatory score for each group were calculated using six random microscopic fields at (40×) magnification.

Some lung paraffin sections from each group were dyed with MT stain and photographed at

Arq. Bras. Med. Vet. Zootec., v.75, n.5, p.857-871, 2023

859

(40×) power (Silva *et al*., 2020). Masson's trichrome staining turns collagen fiber blue, cytoplasm, muscle, and erythrocytes pink, and nuclei dark brown to black (Zhou and Moore, 2017). ImageJ software was utilized to calculate the optical density of Masson's trichrome-stained collagen fiber.

Some paraffin sections of lungs from each group were stained with Alcian blue-PAS stain (Bancroft and Gamble, 2013). The stained sections were photographed at high magnification power (40×). Acid mucin was dyed blue, whereas neutral mucin was dyed magenta. Image analysis software was used to measure mucin content in the lung across ten fields/each group.

In each group, lung sections were stained with anti-PCNA stain and photographed under high magnification (40×). Streptavidin-biotin immunoperoxidase complex staining was utilized for immunohistochemical staining. The positive reaction for PCNA appears as a brown nuclear reaction (Ahmed *et al*., 2019).

For the evaluation of the ultra-structural characteristics of the bronchiolar Clara cells in the lung of various groups, transmission electron microscopy (TEM) processing was done (Graham and Orenstein, 2007). A portion of the lung was immediately fixed in cold glutaraldehyde (5%) for 24 hours, washed three times in 0.1 ml of phosphate-buffer (pH 7.2), and then post-fixed for 1.5 hours with 1 percent osmium tetroxide. The specimens were then dehydrated at various alcohol concentrations and implanted in epoxy resin following a second rinse in phosphate buffer. To evaluate the area that had been cut extremely thinly, semi-thin slices (1 micrometer thick) were made using an LKB ultratome, toluidine blue was added to them, and they were then examined under a light microscope. At the center, Regional Mycology and Biotechnology of Al-Azhar University in Cairo, Egypt, the ultra-thin slices were observed by using a transmission electron microscope (TEM) (JEOL1010 EX II, Japan).

Mean area-percentage of mucin, collagen fiber as well as PCNA positive reactions in ten non-overlapping high-power fields (40×) of paraffinized sections of lungs per each group were measured and statistically evaluated using image analysis software (Imagej version, 1.46).

Version 25 of the Statistical Package for the Social Sciences (SPSS) was utilized to conduct a statistical analysis of all numerical data. The post-hoc Tukey's test was utilized to calculate whether there were any significant differences among groups, and one-way analysis of variance (ANOVA) was utilized to compare the means of multiple groups. If the p value was less than 0.05, the outcome was deemed statistically significant.

RESULTS

The CONT group had normal lung histo-architecture in male albino rats. The murine lung was made up of a terminal bronchiole, an alveolar duct, an alveolar sac, and regular-sized alveolar spaces that were separated by a thin inter-alveolar septum and thick interstitial tissue (Fig. 1A). The LAD group had abnormal structure of lung tissue, with infiltrative papillary bronchiolar adenocarcinoma growing as a tumor lesion invading and obliterating the lumen of terminal bronchiole. The tumor mass was made of irregular papillae lined by hyperplastic columnar epithelial cells together with basal vesicular nuclei and some pleomorphic cells that differed in shape and size (Fig. 1B). The LAD+CMLE treated group had no tumor mass and a terminal bronchiole lined by some hyperchromatic low columnar cells (Fig. 1C). The LAD+CIPL-treated group had no tumor mass in the folded terminal bronchiole, and RBC extravasation was found in the air gaps (Fig. 1D). Cisplatin treatment left some lung lesions in the form of RBC extravasation after treatment of lung cancer bearing rats while CMLE treatment restored of normal lung histology when both treatments compared to control rats thus, CMLE treatment is preferable and safer than Cisplatin treatment.

The semi-quantitative evaluations of lung histo-scoring for bronchiolar wall, alveolar lumen diameter, and inflammatory score among the study groups were shown in table (1) and figure (2). The mean bronchiolar wall thickness in the LAD group (96.20 6.37) was substantially higher than in the CONT group. When compared to the LAD group, CMLE treated and CIPL treated (34.05±2.38) groups significantly reduced the mean bronchiolar wall thickness (Fig. 2A). The alveolar lumen diameter in the LAD group (18.30±1.15) was substantially smaller than in the CONT group (39.14 3.41). The treatment

860

Arq. Bras. Med. Vet. Zootec., v.75, n.5, p.857-871, 2023

with CMLE (35.60±3.35) and CIPL (40.24±5.14) increased the alveolar lumen diameter significantly as compared with the LAD group (Fig. 2B). Furthermore, inflammatory cell scoring in the LAD group (4.00 0.38) was substantially higher than in the CONT group (1.04±0.27). When compared to the LAD group, CMLE (1.78±0.33) and CIPL (2.42 0.19) treated groups significantly reduced inflammatory cell

infiltration (Fig. 2C). Cisplatin treatment resulted in higher values of bronchiolar wall thickness, alveolar lumen diameter, and inflammatory score than CMLE treatment after treatment of lung cancer bearing rats when both treated groups compared to control group therefore, CMLE treatment is preferable in amelioration of pathological changes associated with lung cancer induction in male albino rats.

Table 1. Histology scoring of bronchiolar wall thickness, alveolar lumen diameter and inflammatory score in the study groups

Scoring Groups	Bronchiolar wall thickness (μm)	Alveolar lumen diameter(μm)	Inflammatory score
CONT	32.20±1.22	39.24±1.45	1.03±0.10
LAD	96.20±2.85[*]	18.30±0.51[*]	4.00±0.17[*]
LAD+CMLE	32.03±1.19[#]	35.60±1.49[#]	1.78±0.14[#]
LAD+CIPL	34.05±0.96[#]	40.24±2.12[#]	2.42±0.08[*#]

Values are Mean ± S.E.M. *: significance against CONT group, #: significance against LAD group, $P < 0.05$.
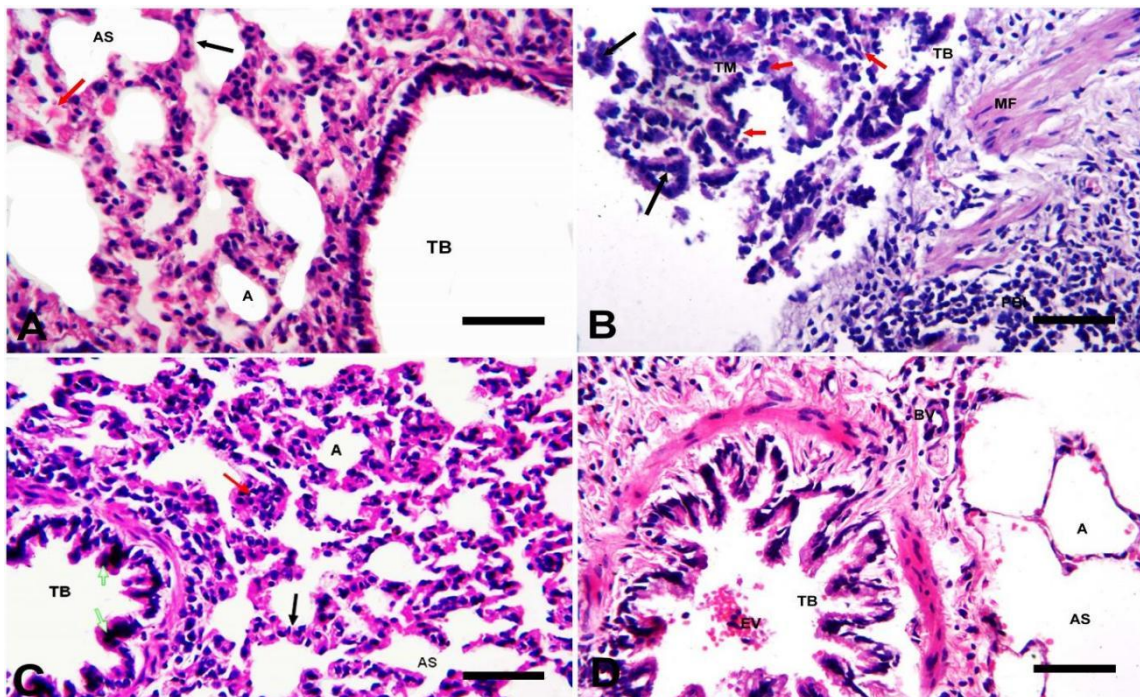

Figure 1. Cross section of rat lung in the study groups (H&E stain). **(A)** CONT group showed normal histo-architecture of lung including terminal bronchiole (TB), alveolar sac (AS), alveoli (A), thin inter-alveolar septum (black arrow) and thick interstitial tissue (red arrow). **(B)** LAD group showed bronchiolar papillary adenocarcinoma exhibited well-defined tumor mass (TM) formed of irregular papillae lined by hyperplastic columnar epithelial cells (black arrow) with basal vesicular nuclei in the epithelial lining of terminal bronchiole (TB) and some pleomorphic that different in their shape and size (red arrows), terminal bronchiole supported by hypertrophied discontinuous muscle fiber (MF) layer and surrounded by peri-bronchiolar inflammation (PBI). **(C)** LAD+CMLE treated group showed terminal bronchiole (TB) that lined with some hyper-chromatic low columnar cell (white arrows), many alveoli (A) separated by thin inter alveolar septum (black arrow) and by thick interstitial tissue (red arrow). **(D)** LAD+CIPL treated group showed folded terminal bronchiole (TB), extravasation (EV) of RBCs in bronchiolar lumen, alveolar sac (AS), alveoli (A), blood vessel (BV). Bar= 50 μm.
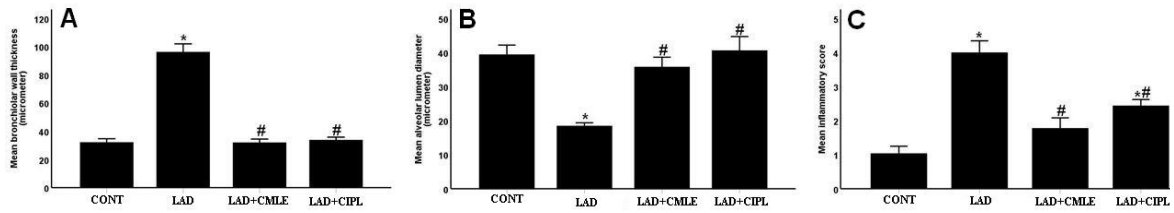
Figure 2. Semi-quantitative evaluations of lung histo-scoring of: **(A)** the bronchiolar wall thickness, **(B)** Alveolar lumen diameter and **(C)** Inflammatory score in H&E stained lung sections in different study groups. The data are expressed as the mean ± S.E.M. *: significance against CONT group, #: significance against LAD group. P < 0.05.

The morphometric area percent of collage fibers, mucin content and PCNA positive immune reaction in the study groups were shown in Table 2 and Figure 3. The collagen fiber area % in the LAD group increased significantly as compared with the CONT group. When compared to the LAD group, rats in the CMLE and CIPL groups had a significant decrease in collagen fiber area percent. When compared to the CONT group, the LAD group showed a substantial increase in the

area percent of total mucins. When compared to the LAD group, rats in the CMLE and CIPL groups had a significantly lower area percent of total mucins. When compared to the CONT group, the LAD group demonstrated a substantial increase in the area percent of PCNA positive reaction. When compared to the LAD group, rats in the CMLE and CIPL groups had a significantly lower area percent of PCNA.

Table 2. Area percent of collagen fiber, AB-PAS positive reaction and PCNA Positive immunoreaction in the study groups

Area Groups	Collagen fiber	AB-PAS positive reaction	PCNA positive immunoreaction
CONT	5.182±0.372	34.771±1.335	5.211±0.540
LAD	16.752±1.462[*]	51.356±1.216[*]	22.932±1.179[*]
LAD+CMLE	7.787±0.752[#]	35.249±2.788[#]	6.235±0.660[#]
LAD+CIPL	7.937±0.241[#]	37.258±1.624[#]	9.37±0.680[#]

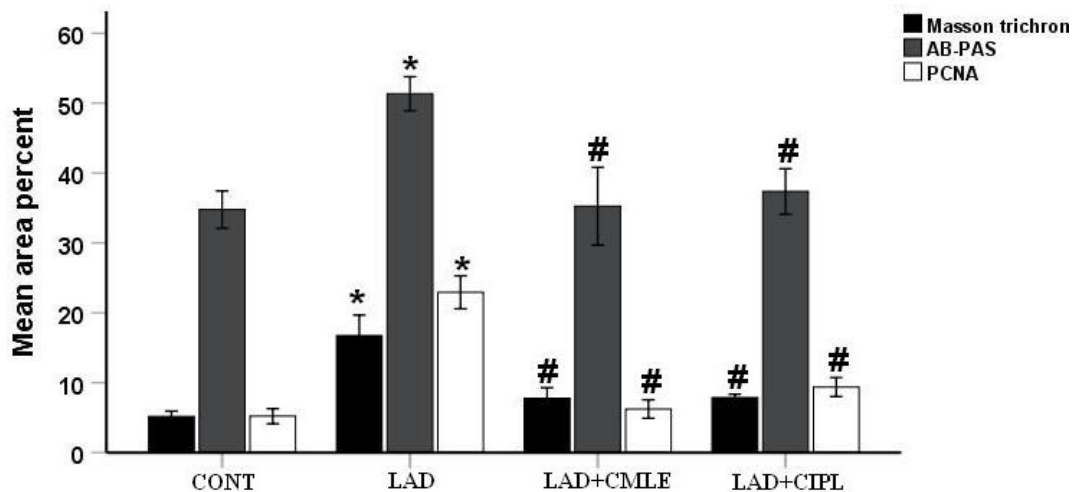Values are Mean ± S.E.M. *: significance against CONT group, #: significance against LAD group, P < 0.05.

Figure 3. Quantitative analysis of mean area percent of Masson trichrome-stained collagen fibers, AB-PAS positive reaction and PCNA positive immunoreaction in the lung of different groups. Values are mean ± S.E.M. *: significance against CONT group, #: significance against LAD group. P < 0.05.

Cisplatin treatment resulted in higher values of collagen fibers content, AB-PAS positive reaction, and anti-PCNA positive immunoreaction than CMLE treatment when both treated groups compared to control group therefore, CMLE treatment is preferable in amelioration of lung fibrosis, high mucin production and higher cellular proliferation associated with lung cancer in male albino rats.

Blue collagen fibers were distributed normally within interstitial tissue and around the terminal bronchiole in the CONT group (Fig. 4A). The LAD group had an aberrant distribution of collagen fibers around and within the terminal bronchiole wall (Fig. 4B). The LAD+CMLE-treated group had moderate collagen fiber deposition around the terminal bronchiole and

between alveoli (Fig. 4C). The LAD+CIPL-treated group had moderate collagen fiber deposition in the terminal bronchiole and between the alveoli (Fig. 4D).

The AB-PAS reaction for total neutral mucinous substance was moderately positive in the CONT group (Fig. 5A). The LAD group demonstrated a robust positive AB-PAS reaction for neutral mucin surrounding the terminal bronchiole and acidic mucin within the tumor mass and the epithelial lining of the terminal bronchiole (Fig. 5B). The LAD+CMLE group had a moderately positive AB-PAS reaction for total neutral mucin (Fig. 5C). The LAD+CIPL group had a moderate positive AB-PAS reaction of total neutral mucin content (Fig. 5D).
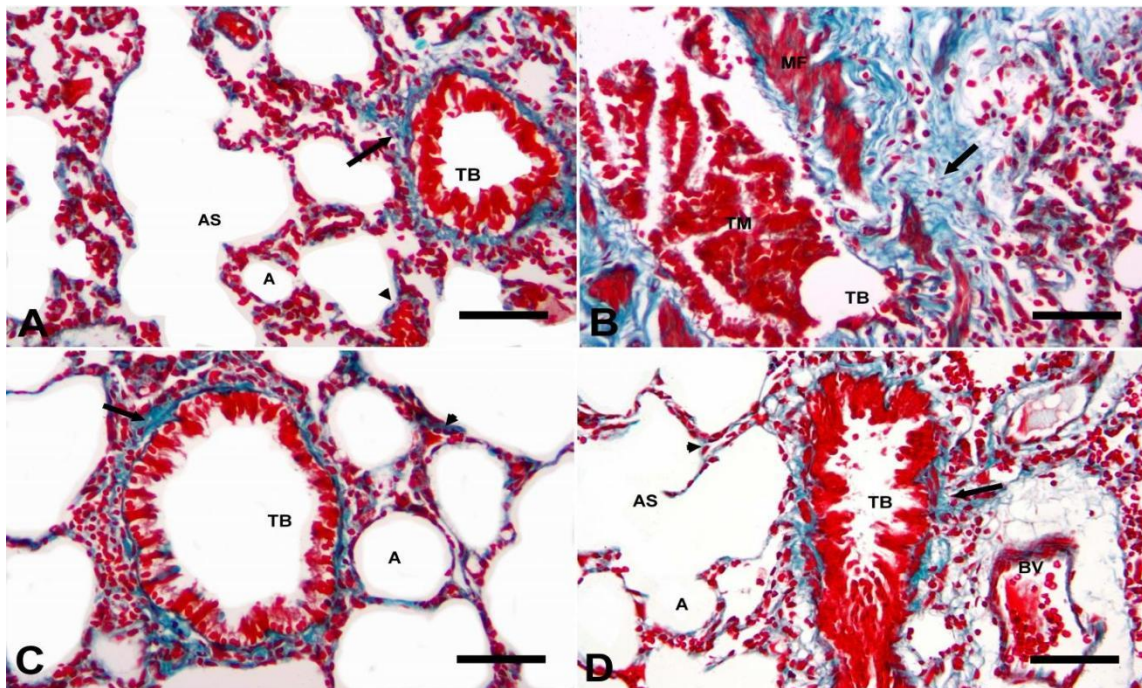

Figure 4. Photomicrograph of transverse section in lung of different groups stained with Masson trichrome. **(A)** CONT group showed normal distribution of minimal amount of blue collagen fibers between lung alveoli (A) , alveolar sac (AS) (arrow head) and around terminal bronchiole (TB) (arrow). **(B)** LAD group showed abnormal distribution of excessive amount of collagen fibers around and within wall of terminal bronchiole (TB) (black arrow), terminal bronchiole (TB) lined with tumor mass (TM) surrounded by disrupted layer of smooth muscle fibers (MF). **(C)** LAD+CMLE treated group showed moderate collagen fiber deposited around terminal bronchiole (TB) (black arrow) and in between alveoli (A) (arrowhead). **(D)** LAD+CIPL treated group showed moderate collagen fiber deposited around slightly folded terminal bronchiole (TB) (black arrow) and in between alveoli (A) (arrowhead). Thick congested blood vessels (BV) existed. Bar = 50μm.
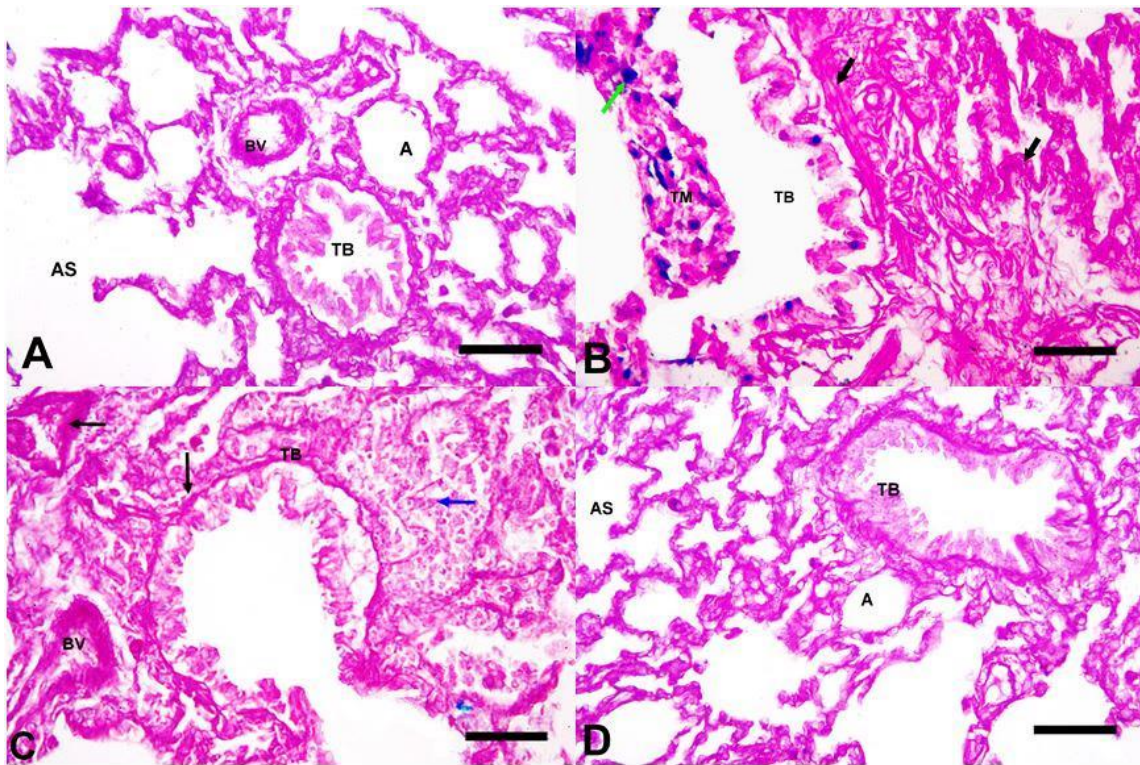
Figure 5. Photomicrographs of transverse sections in lung showed different AB-PAS positive reactions among the study groups (AB-PAS reaction). **(A)** CONT group showed moderate positive AB-PAS reaction of total neutral mucinous substance. Terminal bronchiole (TB), alveolar sac (AS), alveoli (A), blood vessel (BV) present in lung parenchyma. **(B)** LAD group showed strong positive AB-PAS reaction of total mucinous granules for neutral mucins (black arrow) around terminal bronchiole (TB) (black arrow) and for acidic mucins (green arrow) within tumor mass (TM) and epithelial lining of TB. **(C)** LAD+CMLE treated group showed moderate positive AB-PAS reaction for total neutral mucins. Black arrow points for area of strong Rx around (TB) and (BV) while blue arrow for area of moderate Rx in interstitial tissue. **(D)** LAD+CIPL treated group showed moderate positive AB-PAS reaction for staining of total neutral mucins. Bar = 50µm.

In the entire section, the CONT group demonstrated an overall mild to moderate positive immunoreaction for staining of PCNA in the lung (Fig. 6A). The LAD group had overall strong positive PCNA immune reactivity in the lung (Fig. 6B), emphasizing cellular proliferation as a hallmark of cancer progression in the lung. In lung sections, the LAD+CMLE group had a net moderate positive PCNA immunoreaction (Fig. 6C). In the section, the LAD+CIPL treated group demonstrated a moderate positive PCNA total immunoreaction (Fig. 6D).

An ultrathin section of a lung terminal bronchiole from the CONT group revealed normal bronchiolar epithelium consisted of Clara cells and ciliated cells. Clara cells had a primary body and a projecting apex pointing toward the lumen. Clara cell's apex included several pale mitochondria and a few dense secretory granules, while the major body was composed of a notched central nucleus surrounded by scattered spherical or elongated mitochondria, many electron dense secretory granules, and smooth endoplasmic reticulum (Fig. 7A).

The LAD group had abnormally proliferating Clara cells in the terminal bronchiole epithelial lining, resulting in a tumor mass of tightly packed pleomorphic cells identified as Clara cells by dense secretory granules. The nuclei of these cells were pleomorphic and surrounded by vacuolated pale cytoplasm. Most cells did not rest on the basement membrane (Fig. 7B). The LAD group's high magnifications revealed some pleomorphic Clara cells creating a tumor mass

864

Arq. Bras. Med. Vet. Zootec., v.75, n.5, p.857-871, 2023

with deformed cell borders, each cell contained pleomorphic nuclei surrounded by vacuolated cytoplasm, dilated smooth endoplasmic reticulum, and a few secretory granules (Fig. 7C).

The LAD+CMLE treatment group improved the ultrastructure of Clara cells, which are supported by a thick basement membrane. Clara cells had multiple electron rich secretory granules at the apex, whereas the main body consisted of a club-

shaped nucleus surrounded by basal rough endoplasmic reticulum and apical elongated mitochondria (Fig. 7D). The LAD+CIPL-treated group restored the ultrastructure of Clara cells to lesser degrees. Clara cells protruded far into the lumen, enveloping neighboring ciliated cells. Clara cells had a lobed nucleus surrounded by apical dilated smooth endoplasmic reticulum, several electron dense secretory granules, and some Mitochondria in their main body (Fig. 7E).
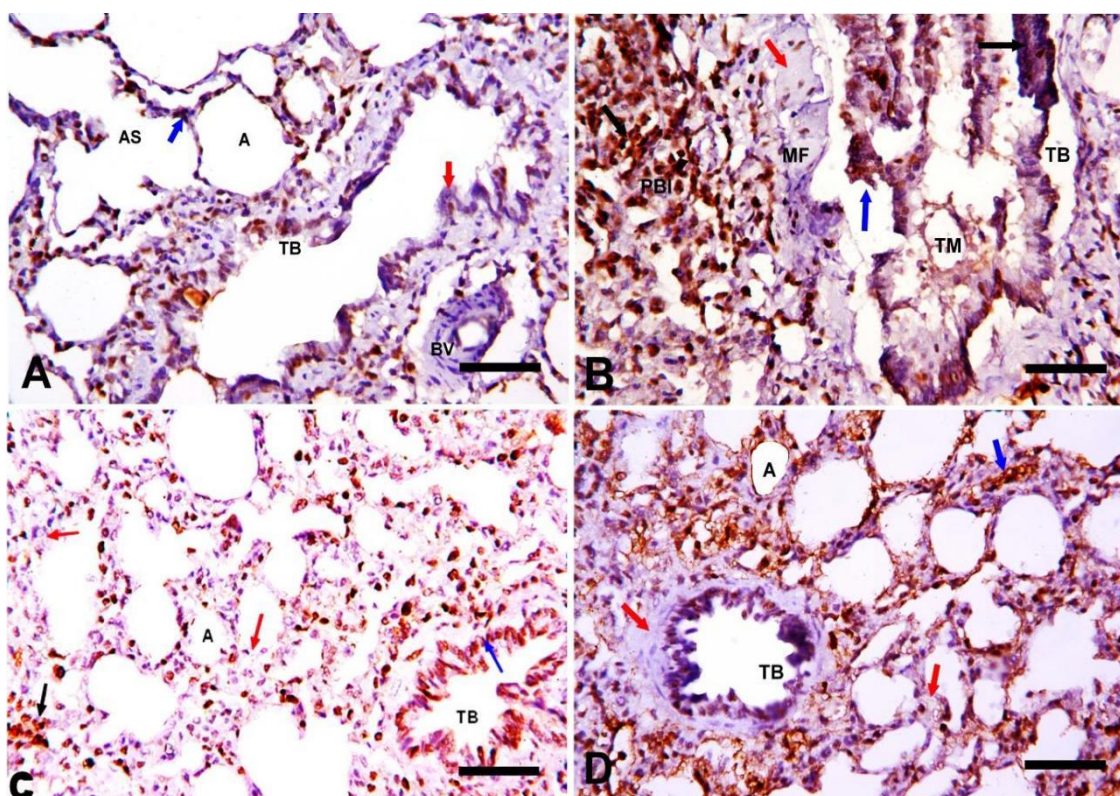

Figure 6. Sections in lung showed different anti-PCNA immunohistochemical reactions in lung cells nuclei of different groups. **(A)** CONT group showed moderate PCNA positive immunoreaction. A moderate reaction (blue arrow) appeared in interstitial cells among alveolar sacs (AS) and alveoli while mild reaction (red arrow) appeared in in some cells of terminal bronchiole (TB). **(B)** LAD group showed strong PCNA positive immunoreaction. Differentially, the strong positive reaction (black arrow) appeared in some cells of tumor mass (TM) occupying terminal bronchiole (TB) lumen and in nuclei of peri-bronchiolar inflammatory cells (PBI) whilst moderate reaction in some cells of (TM) but weak PCNA positive reaction found in muscle layer of (TB). **(C)** LAD+CMLE treated group showed moderate PCNA positive immunoreaction. Differentially, strong reaction (black arrow) appeared in few interstitial cells among alveoli (A), moderate reaction (blue arrow) in bronchiolar epithelial cells of terminal bronchiole (TB) whilst weak reaction (red arrow) appeared in many interstitial cells. **(D)** LAD+CIPL treated group showed moderate PCNA positive immune reactivity. Differentially, moderate reaction (blue arrow) in in some interstitial cells whilst weak reaction (red arrow) appeared in wall of terminal bronchiole and in some interstitial cells. Bar = 50μm.
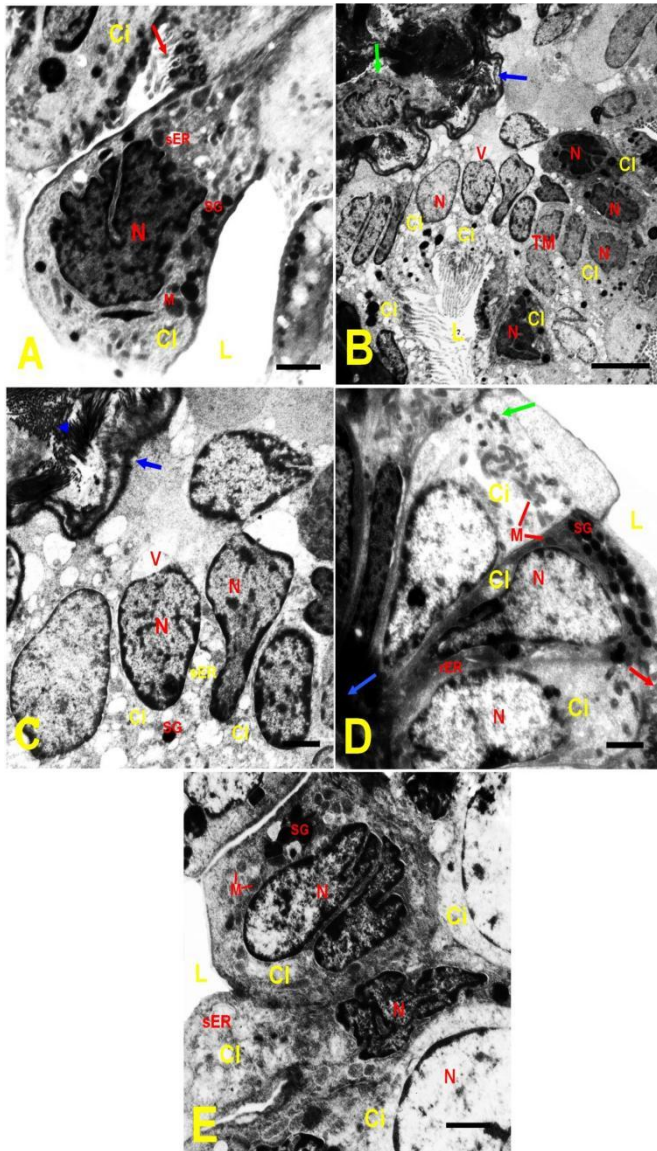
Arq. Bras. Med. Vet. Zootec., v.75, n.5, p.857-871, 2023

865

Figure 7. Electron micrograph of part of epithelial lining of terminal bronchiole mainly Clara cells in all study groups. **(A)** CONT group showed a part of bronchiolar epithelium lining terminal bronchiole comprising ciliated cells (Ci) and Clara cells (Cl). Clara cells consisted of main body and protruding apex toward lumen (L). Apex of Clara cell contained some pale mitochondria (M), dense secretory granules (SG). The main body of Clara cell formed of notched central nucleus (N) which surrounded by cytoplasmic organelles such as some scattered .

spherical or elongated mitochondria (M), electron dense secretory granules (SG) and smooth endoplasmic reticulum (sER). Ciliated cells have cilia (red arrow) directed toward airway lumen. **(B)** LAD group showed proliferated Clara cells (Cl) of terminal bronchiole forming tumor mass (TM) of closely packed group of pleomorphic cells with obliterated lumen (L). Clara cells possessed a pleomorphic nucleus (N) surrounded by vacuolated pale cytoplasm (v). Most cells of epithelial layer did not rest on basement membrane (blue arrow) beneath it, hypertrophied fibrocyte (green arrow) was existed below. The ciliated cells (Ci) were compressed greatly by adjacent enlarged neoplastic Clara cells. **(C)** A magnified part of the previous section of LAD group showed some pleomorphic Clara cells (Cl) forming tumor mass with distorted cell boundaries, each consisted of pleomorphic nuclei (N) surrounded by pale vacuolated cytoplasm (v), dilated smooth endoplasmic reticulum (sER) and few residual dense secretory granules (SG). The basement membrane (blue arrow) and its underlying fibrin deposits (green arrow) existed. **(D)** LAD+CMLE treated group showed ameliorated ultrastructure of ciliated cell (Ci) and Clara cell (Cl) which rest on thick basement membrane (blue arrow). The apex of Clara cell contained many electron dense secretory granules (SG). The main body of Clara cell formed of club-shaped nucleus (N) that surrounded by basal rough endoplasmic reticulum (rER) and apical elongated mitochondria (M). The lower ciliated cells have cilia (red arrow) run toward airway lumen (L) while the upper cell appeared with detached cilia with remaining basal bodies (green arrow). **(E)** LAD+CIPL treated rats group showed more or less restoration of ultra-structure of ciliated cells (Ci) and Clara cells (Cl). Clara cells protruded much into lumen (L) covering adjacent ciliated cells. The main body Clara cell contained lobed nucleus (N) surrounded by apical dilated smooth endoplasmic reticulum (sER), many electrons dense secretory granules (SG) some Mitochondria (M). Bar = 500 nm excluding figure B = 2 μm.

Regarding TEM, CMLE treatment resulted in improved the ultrastructure of Clara cells than Cisplatin with some lesions when both treated groups compared to control group therefore, CMLE treatment is preferable in amelioration of ultra-structural features of Clara cells forming this type of lung cancer in male albino rats.

The above results showed that Cisplatin treatment left some lung lesions in the form of RBC extravasation after treatment of lung cancer bearing rats while CMLE treatment restored normal lung histology when both treatments compared to control rats. Moreover, CMLE treatment resulted in ameliorated values of

bronchiolar wall thickness, alveolar lumen diameter, inflammatory score, collagen fibers content, AB-PAS positive reaction, and anti-PCNA positive immunoreaction than Cisplatin treatment when both treated groups compared to control group. Therefore, CMLE treatment allows a new alternative along with less toxicity than the Cisplatin drug in lung-cancer therapy.

DISCUSSION

The induced lung-cancer model employed in this study was the same as that used by Radwan *et al.* (2021) who had used 4 intraperitoneally injections of ethyl carbamate 0.375 g/kg over a 12-week period with a three week gap between treatments. Janker *et al.* (2018) determined that three times of ethyl carbamate injection (1 mg/gm in one week) induced significantly more tumor nodules than one-time injection in mice, despite 0% death and morbidity and 100% tumor incidence rate. In the experimental paradigm, the length of time the animals were given to ethyl carbamate determines the induction of adenocarcinoma (Stakisaitis *et al.*, 2014).

The ethyl carbamate's carcinogenic activity in our model could be attributed to the formation of vinyl carbamate, an active metabolite, which is a strong mutagen and stimulates the formation of electrophilic species that which interacts by DNA to generate 2-oxoethyl adducts as vinyl chloride (Ding *et al.*, 2014).

Ethyl Carbamate injection caused progressive bronchiolar adenocarcinoma, which manifested as a tumor lesion infiltrating and partially obliterating the lumen of terminal bronchiole. The tumor mass was made up of hyperplastic columnar epithelial cells together with basal vesicular nuclei and pleomorphic cells with different cell sizes and shapes. According to the recent study, the bronchiolar adenocarcinoma cells' nuclei were pleomorphic, in addition to frequent mitosis, penetration of tumor cell into bronchiolar lumen, and wall push on the surrounding tissues, these pathologic features was in accordance with Stakisaitis *et al.* (2015) observations.

According to Gurukumar *et al.* (2010), the ethanolic leaf extract of *C. alata* displayed good anticancer effectiveness against generated cancer

of prostate appearing in *In vivo* models utilizing N-methyl N-nitrosourea and Testosterone.

The existence of observable lesions in the LAD+CIPL treated group, for example RBC extravasation and inflammation in airway spaces, may be attributed to Cisplatin, which is not selective for cancer-cells and affects normal-cells as well (Sak, 2012).

Collagen fibers increased significantly in the LAD group compared toward the CONT group, confirming the findings of Anandakumar *et al.* (2015) who discovered enhanced collagen deposition in lung cancer-induced mice. The high collagen fiber content in the lung cancer group could be attributable to immunological and inflammatory processes that cause fibroblast activation and collagen deposition (Zidan, 2011). The current study suggests that the improvement in collagen fibers after CMLE treatment may be due to CMLE's anti-inflammatory characteristics (Patrick-Iwuanyanwu *et al.*, 2011).

The Alcian blue-PAS method is a straightforward method for identifying and characterizing muco-substances in tissue slices that appear to distinguish clearly between acid and neutral mucins (Ionilă *et al.*, 2011). Chronic mucus hypersecretion has been displayed to be a significant predictor of lung cancer death (Lange *et al.*, 1990). In this work, CMLE therapy restored normal mucin content in lung cancer-bearing rats.

PCNA, proliferating cell nuclear antigen, is indeed a marker of cell proliferation (Naryzhny, 2008). PCNA seems to be a nuclear peptide with 36 kDa molecular weight that has been labeled as a DNA polymerase delta auxiliary protein (Nanji and Tahan, 1996). The terminal bronchiolar lining cell's nuclei as well as inflammatory peri-bronchiolar cells strongly responded positively to PCNA in the present study, significantly increasing the area% of PCNA in the LAD group as compared to the CONT group. This finding was supported by Wang *et al.* (2018) who demonstrated that expression of PCNA was raised in NSCLC tissues and cells and that overexpression of PCNA in lung-cancer cells led to proliferation of cells, clonal formation, along with tumor growth. In the current study, rats given CMLE had a moderate PCNA positive reaction in the lung. This discovery could be

attributed to CMLE's anti-proliferative properties (Modarresi Chahardehi *et al*., 2021).

Cisplatin anticancer efficacy in the present work was consistent with Hamzawy *et al*. (2022) who revealed that carboplatin treatment of urethane-induced lung cancer in BALB/C mice was substantially improved in all molecular, biochemical, and histological studies.

The lung cancer in this investigation is made up of neoplastic Clara cells. This conclusion was compatible with Reznik-Schuller (1976) who observed that long-term administration of nitrosamine derivatives to hamster rats, results in the production of bronchogenic carcinomas composed of neoplastic Clara cells. Tumor cells of the Clara cell type have a cluster of electron-dense secretory granules, whereas tumor cells of the type II alveolar epithelial cell type have lamellar inclusion bodies inside the cytoplasm (Hou *et al*., 2020).

Clara cells of the LAD group had abundant secretory vesicles at the apex, pleomorphic nuclei, peri-nuclear rough endoplasmic reticulum, vacuolated cytoplasm, and dilated smooth endoplasmic reticulum with flocculent material. The altered ultrastructure of Clara cells forming tumor mass in this work was consistent with Van Winkle *et al*. (1999) who formed that following acute naphthalene injury of bronchiolar Clara cells *In vivo*, the early phases of Clara cell injury as smooth endoplasmic reticulum swelling, and bleb development preceded the rise in permeability of cell membrane. The following major events occur during acute injury of Clara cell *in vivo*: cytoplasmic apical blebbing, cytoplasmic vacuolization, SER swelling, and permeability of cell membrane which markedly by exfoliation of apical parts of injured Clara cells into airway lumen.

Phimister *et al*. (2005) found that significant GSH depletion produces significant swelling, actin cytoskeleton disturbances, and plasma membrane blebbing in Clara cells, which explains the altered ultrastructure of Clara cells in ethyl carbamate-induced adenocarcinoma. These cellular alterations have been seen in cells exposed to a variety of toxins and may represent a general cell response to GSH depletion and/or oxidative stress that occurs during the early stages of cell death (Manygoats *et al*., 2002).

Blundell (2006) confirmed our Clara cell findings by observing nuclear chromatin margination and clumping, mitochondrial swelling, endoplasmic reticulum dilation, Clara cells become enlarged, and numerous vacuoles form adjacent to the cellular membranes after toxic substances enter the lungs via inhaled air. Clara cells are thought to be vital in protecting the airways from the negative effects of a hazardous external environment (Reynolds and Malkinson, 2010). The extract's anti-proliferative action may be responsible for the positive impact of CMLE treatment on bronchiolar Clara cell ultrastructure found in this investigation (Modarresi Chahardehi *et al*., 2021).

CONCLUSION

The treatment of lung cancer bearing rats with *C. alata* leaf extracts showed restoration of almost normal lung histoarchitecture and decreased lung inflammation, mucin production, cell proliferation while Cisplatin treatment resulted in some restoration of normal lung histoarchitecture and decreased lung inflammation, mucin production, cell proliferation to a lower extent than CMLE treatment. Thus, *C. alata* leaf extract should be utilized as a novel foundation of anticancer natural compound against lung-cancer. Therefore, the current study concluded that CMLE treatment delivers a new alternative with less toxicity than Cisplatin drug in lung cancer therapy. This work is limited to histology and ultrastructural levels, and additional study is needed.

ACKNOWLEDGMENTS

868

Arq. Bras. Med. Vet. Zootec., v.75, n.5, p.857-871, 2023

REFERENCES

ADEDAYO, O.; ANDERSON, W.A.; MOO-YOUNG, M. *et al.* Phytochemistry and antibacterial activity of Senna alata flower. *Pharm. Biol.*, v.39, p.408-412, 2001.

AHMED, R.F.; MOUSSA, R.A.; ELDEMERDASH, R.S.; ZAKARIA, M.M.; ABDEL-GABER, S.A. Ameliorative effects of silymarin on HCl-induced acute lung injury in rats, role of the Nrf-2/HO-1 pathway. *Iran J. Basic Med. Sci.,* v.22, p.1483-1492, 2019.

ALI, M.I.; ABOUL-ENEIN, A.M.; MOHAMED, S.M. *et al.* Phytochemical, cytotoxicity and antioxidant investigation of Cassia alata leaves growing in Egypt. *J. Innov. Pharm. Biol. Sci.*, v.4, p.97, 2017.

AL-MAJED, A.A. Carnitine deficiency provokes cisplatin-induced hepatotoxicity in rats. *Basic Clin. Pharmacol. Toxicol.*, v.100, p.145-150, 2007.

ANANDAKUMAR, P., KAMARAJ, S., JAGAN, S. *et al.* The anticancer role of capsaicin in experimentally induced lung carcinogenesis. *J. Pharmacopuntura*, v.18, p.19-25, 2015.

BANCROFT, J.D.; GAMBLE, M. *Theory and practice of histological techniques*. 6.ed. New York: Churchill Livingstone, 2013. p.125-158.

BANCROFT, J.D.; LAYTON, C. The hematoxylin and eosin. In: SUVARNA, S.K.; LAYTON, C.; BANCROFT, J.D. (Eds.). *Bancroft's theory and practice of histological techniques*. 8.ed. Philadelphia: Elsevier, 2019. p.126-138.

BLUNDELL, P. The biology of Clara cells - review paper. *Int. J. Mol. Med. Adv. Sci.*, v.2, p.307-311, 2006.

DENNIS, M.J.; HOWARTH, N.; KEY, P.E.; POINTER, M.; MASSEY, R.C. Investigation of ethyl carbamate levels in some fermented foods and alcoholic beverages. *Food Addit. Contam.*, v.6, p.383-389, 1989.

DING, Y.; XUAN, W.; CHEN, C. *et al.* Differences in carcino-embryonic antigen levels between colon and rectal cancer. *Mol. Clin. Oncol.*, v.2, p.618-622, 2014.

DONG, C.; WANG, G.; LI, B. *et al.* Anti-asthmatic agents alleviate pulmonary edema by upregulating AQP1 and AQP5 expression in the lungs of mice with OVA-induced asthma. *Respir. Physiol. Neurobiol.*, v.181, p.21-28, 2012.

FERNAND, V.E.; LOSSO, J.N.; TRUAX, R.E. *et al.* Rhein inhibits angiogenesis and the viability of hormone-dependent and -independent cancer cells under normoxic or hypoxic conditions in vitro. *Chem. Biol. Interact.*, v.192, p.220-232, 2011.

GRAHAM, L.; ORENSTEIN, J.M. Processing tissue and cells for transmission electron microscopy in diagnostic pathology and research. *Nat. Protoc.*, v.2, p.2439-2450, 2007.

GURUKUMAR, D.; RATHI, M.A.; MEENAKSHI, P. *et al.* Anticancer activity of Cassia senna (L) against prostate carcinogenesis. *J. Pharm. Res.*, v.3, p.3028-3031, 2010.

HAMZAWY, M.A.; ABO YOUSSEF, A.M. An additional risk of lung cancer from recurrent exposure to ethyl carbamate (EC) in BALB/C Mice. *J. Cancer Sci. Ther.*, v.7, p.11, 2015.

HAMZAWY, M.A.; ABO-YOUSSEF, A.M.; MALAK, M.N.; KHALAF, M.M. Multiple targets of Nrf 2 inhibitor, trigonelline in combating urethane-induced lung cancer by caspase-executioner apoptosis, cGMP and limitation of cyclin D1 and Bcl2. *Eur. Rev. Med. Pharmacol. Sci.,* v.26, p.9393-9408, 2022.

HOU, W.L.; CHANG, M.; LIU, X.F.; HU, L.S.; HUA, S.C. Proteomic and ultrastructural analysis of Clara cell and type II alveolar epithelial cell-type lung cancer cells. *Transl. Cancer Res.*, v.9, p.565-576, 2020.

IBRAHIM, A.S.; KHALED, H.M.; MIKHAIL, N.N.; BARAKA, H.; KAMEL, H. Cancer incidence in egypt: results of the national population-based cancer registry program. *J. Cancer Epidemiol.*, v.2014, p.437971, 2014.

IONILĂ, M.; MARGARITESCU, C.L.; PIRICI, D.; MOGOANTA, S.S. Mucinoous adenocarcinoma of the colon - a histochemical study. *Rom. J. Morphol. Embryol.*, v.52, 783-790, 2011.

JAFRI, S.; GLASS, J.; SHI, R.M.D.P.; PRINCE, M.; KLEINER-HANCOCK, H. Thymoquinone and cisplatin as a therapeutic combination in lung cancer: in vitro and in vivo. *J. Exp. Clin. Cancer Res.*, v.29, p.87, 2010.

Arq. Bras. Med. Vet. Zootec., v.75, n.5, p.857-871, 2023

869

JANKER, F.; WEDER, W.; JANG, J.H.; JUNGRAITHMAYR, W. Preclinical, non-genetic models of lung adenocarcinoma: a comparative survey. *Oncotarget*, v.9, p.30527-30538, 2018.

JONGH, F.E.; VAN VEER, R.N.; VELTMAN, S.J. *et al*. Weekly high-dose cisplatin is a feasible treatment option: analysis on prognostic factors for toxicity in 400 patients. *Br. J. Cancer*, v.88, p.1199-1206, 2003.

JU, M.H.; KIM, H.R.; KIM, J.B. *et al*. Surgical outcomes in small cell lung cancer. *Korean J. Thorac. Cardiovasc. Surg*., v.45, p.40-44, 2012.

LANGE, P.; NYBOE, J.; APPLEYARD, M.; JENSEN, G.; SCHNOHR, P. Ventilatory function and chronic mucus hypersecretion as predictors of death from lung cancer. *Am. Rev. Respir. Dis*., v.141, p.613-617, 1990.

LEVY, A.; LEWIS, A. Cassia alata leaf extract induces cytotoxicity in A549 lung cancer cells via a mechanism that is caspase 8 dependent. *West Indian Med. J*., v.60, p.608-614, 2011.

LIU, A.; XU, L.; ZOU, Z.; YANG, S. Studies on chemical constituents from leaves of Cassia alata. *Chin. J. Chin. Materia Med*., v.34, p.861-863, 2009.

MANYGOATS, K.R.; YAZZIE, M.; STEARNS, D.M. Ultrastructural damage in chromium picolinate-treated cells: a tem study. Transmission electron microscopy. *J. Biol. Inorg. Chem*., v.7, p.791-798, 2002.

MODARRESI CHAHARDEHI, A.; ARSAD, H.; ZAFIRAH ISMAIL, N.; LIM, V. Low cytotoxicity, and antiproliferative activity on cancer cells, of the plant Senna alata (Fabaceae). *Int. J. Trop. Biol*., v.69, p.317-330, 2021.

MOHAMED, S.; IBRAHIM, M.; SOLIMAN, D. Anti-Cancer role of Cassia alata leaf extract in a rat model of lung cancer. *Sohag J. Sci*., v.8, p.21-28, 2023.

NANJI, A.A.; TAHAN, S.R. Association between endothelial cell proliferation and pathologic changes in experimental alcoholic liver disease. *Toxicol. Appl. Pharmacol.,* v.40, p.101-107, 1996.

NARYZHNY, S.N. Proliferating cell nuclear antigen: a proteomics view. *Cell. Mol. Life Sci.*, v.65, p.3789 -3808, 2008.

OLARTE, E.I.; HERRERA, A.A.; VILLASEÑOR, I.M.; JACINTO, S.D. In vitro antitumor properties of an isolate from leaves of Cassia alata L. *Asian Pac. J. Cancer Prev*., v.14, 3191-3196, 2013.

ONYEGEME-OKERENTA, B.M.; NWOSU, T.; WEGWU, M.O. Investigation of the effect of aqueous leaf extract of Senna alata (l) roxb on palm oil- induced hyper-lipidaemic plasma lipid in wister rats. *Int. J. Clin. Exp. Med. Sci*., v.5, p.19-34, 2017.

PATRICK-IWUANYANWU, K.; ONYEIKE, E.N.; DAR, A. Anti-inflammatory effect of crude methanolic extract and fractions of ring worm plant Senna alata (L. roxb) leaves from Nigeria. *Pharm. Sin*., v.2, p.9-16, 2011.

PHIMISTER, A.J.; WILLIAMS, K.J.; VAN WINKLE, L.S.; PLOPPER, C.G. Consequences of abrupt glutathione depletion in murine Clara cells: ultrastructural and biochemical investigations into the role of glutathione loss in naphthalene cytotoxicity. *J. Pharmacol. Exp. Ther*., v.314, p.506-513, 2005.

RADWAN, E.; ALI, M.; FAIED, S. *et al*. Novel therapeutic regimens for urethane-induced early lung cancer in rats: Combined cisplatin nanoparticles with vitamin-D3. *IUBMB Life*, v.73, p.362-374, 2021.

REYNOLDS, S.; MALKINSON, A. Clara cell: progenitor for the bronchiolar epithelium. *Int. J. Biochem. Cell Biol*., v.42, p.1-4, 2010.

REZNIK-SCHULLER, H. Ultrastructural alterations of nonciliated cells after nitrosamine treatment and their significance for pulmonary carcinogenesis. *Am. J. Pathol*., v.85, p.549-554, 1976.

SAK, K. Chemotherapy and dietary phytochemical agents. *Chemother. Res. Pract*., v.2012, p.1-11, 2012.

SANTARPIA, M.; LIGUORI, A.; KARACHALIOU, N. *et al*. Osimertinib in the treatment of non-small-cell lung cancer: design, development and place in therapy. *Lung Cancer*, v.8, p.109-125, 2017.

SILVA BRUM, I.; FRIGO, L.; LANA DEVITA, R. *et al*. Histomorphometric, immunohistochemical, ultrastructural characterization of a nano-hydroxyapatite/beta-tricalcium phosphate composite and a bone xenograft in sub-critical size bone defect in rat calvaria. *Materials*, v.13, p.4598, 2020.

870

Arq. Bras. Med. Vet. Zootec., **v.75, n.5, p.857-871, 2023**

SPENCER, L.T.; BANCROFT, J.D. Tissue processing. In: SUVARNA, S.K.; LAYTON, C.; BANCROFT, J.D. (Eds.). *Bancroft's theory and practice of histological techniques*. 7.ed. Churchill Livingstone: ExpertConsult.com, 2013. p.105-123.

STAKISAITIS, D., MOZURAITE, R., JUODZIUKYNIENE, N. *et al*. Sodium valproate enhances the urethane-induced lung adenomas and suppresses malignization of adenomas in ovariectomized female mice. *Int. J. Endocrinol.*, v.2015, p.218219, 2015.

STAKISAITIS, D.; ULECKIENE, S.; DIDZIAPETRIENE, J. *et al*. Sodium valproate enhances urethane tumorigenicity in lungs of male but not female mice. *EXCLI J.,* v.13, p.667-687, 2014.

SUNG, H.; FERLAY, J.; SIEGEL, R. L. *et al*. Global cancer statistics 2020: GLOBOCAN estimates of incidence and mortality worldwide for 36 cancers in 185 countries. *CA-Cancer J. Clin.*, v.71, p.209-249, 2021.

SWETHA, G.M.S.; KEERTHANA, C.K.; RAYGINIA, T.P.; ANTO, R.J. Cancer chemoprevention: a strategic approach using phytochemicals. *Front. Pharmacol.*, v.12, p.809308, 2022.

TANRIVERDI, T.; HANIMOGLU, H.; KACIRA, T. *et al*. Glutathione peroxidase, glutathione reductase and protein oxidation in patients with glioblastoma multiforme and transitional meningioma. *J. Cancer Res. Clin. Oncol.*, v.133, p.627-633, 2007.

TRAVIS, W.D. Update on small cell carcinoma and its differentiation from squamous cell carcinoma and other non-small cell carcinomas. *Mod. Pathol.*, v.25, suppl.1, p.S18-S30, 2012.

USMAN, M.; KHAN, W.R.; YOUSAF, N. *et al*. Exploring the phytochemicals and anti-cancer potential of the members of fabaceae family: a comprehensive review. *Molecules*, v.27, p.3863, 2022.

VAN WINKLE, L.S.; JOHNSON, Z.A.; NISHIO, S.J.; BROWN, C.D.; PLOPPER, C.G. Early events in naphthalene-induced acute Clara cell toxicity: comparison of membrane permeability and ultrastructure. *Am. J. Respir. Cell Mol. Biol.*, v.21, p.44-53, 1999.

WANG, L.; KONG, W.; LIU, B.; ZHANG, X. Proliferating cell nuclear antigen promotes cell proliferation and tumorigenesis by up-regulating STAT3 in non-small cell lung cancer. B*iomed. Pharmacother.*, v.104, p.595-602, 2018.

WILCOX, H.B.; AL-ZOUGHOOL, M.; GARNER, M.J. *et al*. Case-control study of radon and lung cancer in New Jersey. *Radiat. Prot. Dosim.*, v.128, p169-179, 2008.

YOUSEF, M.I.; SAAD, A.A.; EL-SHENNAWY, L.K. Protective effect of grape seed proanthocyanidin extract against oxidative stress induced by cisplatin in rats. *Food Chem. Toxicol.*, v.47, p.1176-1183, 2009.

ZHOU, Q.; PAN, H.; LI, J. Molecular insights into potential contributions of natural polyphenols to lung cancer treatment. *Cancers*, v.11, p.1565, 2019.

ZHOU, X.; MOORE, B.B. Lung section staining and microscopy. *Bio. Protoc.*, v.7, p.10, 2017.

ZIDAN, R.A. Effect of long-term administration of amiodarone on rat lung and the possible protective role of vitamin E: a histological and immunohistochemical study. *Egypt. J. Histol.*, v.34, p.117-128, 2011.

Arq. Bras. Med. Vet. Zootec., v.75, n.5, p.857-871, 2023

871